Mg_xZnO_{1-x} photodetector grown by chemical spraying pyrolysis technique

Abdulazeez O. Mousa, Saleem H. Trier

Abstract– **In this research was prepared Mg_xZnO_{1-x}/n-Si photodetector by using chemical spraying pyrolysis (CSP) technique, and different proportions volumetric ofMg-contents (0,30,50,70,and 90)%,at a temperature of (450)°C, were constant thickness by fixing a number sprinkles and was thickness of all films ranges between(80±5)nm, nitrogen gas under pressure (4.5) bar was used. The crystal structure was examined using X-ray diffraction (XRD). The results showed that all the films of polycrystalline. As was studied the topography of the surface of the films by using field emission scanning electron microscopy (FESEM), and energy dispersive X-ray (EDS), where decreases grain size with adding Mg-content. As well as that add MgO in the films lead to a decrease in surface roughness. Also, (EDS) showed that the films contain elements (Si, N, O, Zn, and Mg) as expected. As were studied topography of the surface of the films by using atomic force microscopy (AFM), and showed that the grain size of the ZnO nanostructure depends on the ratio of Mg-content of volumetric, where decreases the grain size with increasing Mg-content. As well as the increase in the proportion of Mg-content in the films lead to a decrease in surface roughness. In this work we studied the spectral properties of the Mg_xZnO_{1-x}/n-Si photodetector, and found that the values of the spectral response, quantum efficiency, and specific detectivity increases and shift toward the wavelengths higher. While the equivalent power of the noise increases randomly, with increase Mg-content.**

***Keywords*— Photodetector, Mg_xZnO_{1-x}, responsivity, quantum efficiency, specific detectivity**

I. INTRODUCTION

Photon detectors are solid- state devices that operate under the influence of photon effects. The photon detectors essentially measure the rate at which quanta are absorbed, thus they respond only to those photon of short wavelength; therefore, their response at any wavelength is proportional to the rate at which photons of wavelength are absorbed. In photon detectors, the radiation is absorbed directly by the electronic system to cause changes in the electrical properties [1]. Photon detectors have small sizes, minimum noise, low biasing voltage, high sensitivity, high reliability, and fast response time [2]. Therefore, they are very useful in optical-fiber communications systems. Basically, if a photon of sufficient energy excites an electron from a non-conducting state into a conducting state, the photoexcited electron will generate current or voltage in the detector. Most photon detectors have a detectivity that is one or two orders of magnitude greater incident photons and the electrons of the detector material. This interaction is called photo effect. Photon detectors include photoconductive (PC), photovoltaic (PV) and photoemissive detectors. That certain materials have the power of changing their resistance at exposure to light. Such materials are known as photoconductors. They represent the first type of semiconductor photon detector. The photoconductive detector consists of a single crystal of semiconductor material of two Ohmic contacts, and a voltage applied between them. The semiconductor is conducting, and therefore some current flows even without light shining on the material (dark current). The incident photon energy creates free carriers in the crystal and changes the conductivity of the material. This type of detector can be used for automatic light control in homes and office buildings to turn light on at dawn and off at dark. Also, they are useful in optical signaling systems. Other types of photoconductivity are possible which are not associated with a change in the free-carrier concentration. For example, when long-wavelength electromagnetic radiation, which does not cause inter band migration and does not ionize impurity center, is absorbed by free carriers, the energy of the carriers is increased. Such an increase leads to a change in carrier mobility and, consequently, to an increase in electrical conductivity. Such secondary photoconductivity decreases at high frequencies and is not frequency dependent at low frequencies. The change in mobility upon exposure to radiation may be caused not only by an increase in carrier energy but also by the effect of the radiation on electron scattering in the crystal lattice [1]. The aims of this paper is to determine the spectral response, quantum efficiency, and the noise equivalent power through the uses of optimal conditions for the prepared Mg_xZnO_{1-x}/n-Si samples to manufacture photodetectors by chemical spray pyrolysis (CSP) technique.

II. THE THEORETICAL PART

There are many parameters affecting the performance of the detectors. These parameters are:

1. Responsivity (R_λ)

(R_λ) is defined as the ratio between the output electrical signals (voltage or current) to the incident radiation power or is defined as the (RMS) signal voltage to the (RMS) value of the incident radiation power. The responsivity for monochromatic light of wavelength incident normally is given by [1].

$$R_\lambda = \frac{I_{ph}}{P_{in}} \quad \text{or} \quad R_\lambda = \frac{V}{P_{in}} \qquad (1)$$

Where I_{ph} photocurrent flowing between the electrodes.

2. Quantum efficiency (QE)

The (QE) is defined as the efficiency with which an incident photon results in the excitation of an electron. It is a normalized value and is equal to the number of electrons excited divided by the number of photons incident on the detector's active area. Therefore, the (QE) of radiation detector is [3]:

$$QE = \frac{h\nu\, I_{ph}}{q\, P_{in}} \quad (2)$$

$$QE = \frac{1240\, R_\lambda}{\lambda_{(nm)}} \quad (3)$$

The QE for an ideal detector is unity.

3. The noise in detectors

The noise is referred to the signal generated in the detector at the absence of the radiation. The relation between dark current and noise current is [4].

$$I_n = (2q\, I_d\, \Delta f)^{1/2} \quad (4)$$

Where (Δf) is bandwidth

4. Detectivity (D) and specific detectivity (D*)

The (D) is defined as the signal-to-noise ratio per unit incident radiation power and it is defined as [2].

$$D = 1/NEP = R_\lambda / I_n \quad (5)$$

Specific detectivity(D*) (normalized detectivity) it is the detector signal-to-noise ratio when one Watt of optical power is incident on the detector with optical area one cm^2 and the noise is measured with a band width of one Hz. It is used because it is normally dependent of the size of the detector and the bandwidth of the measurement circuit while (D) depends on both. The peak value of (D*) at specific wavelength can be written as [2,4].

$$D^* = D (A\, \Delta\, f)^{1/2} \quad (6)$$

Or

$$D^* = R_\lambda (A\, \Delta\, f)^{1/2} / I_n \quad (7)$$

The value depends on the wavelength of the signal radiation and the frequency at which it modulated.

5. Noise equivalent power (NEP)

(NEP) is defined as the root mean square (RMS) incident radiant power falling on the detector that is required to produce an (RMS) signal voltage or current equal to the (RMS) noise voltage or current at the detector output [2]. It is expressed as:

$$NEP = I_n / R_\lambda \quad (8)$$

The detection capability of the detector improves as the (NEP) decreases.

III. THE EXPERIMANTAL PART

The Mg_xZnO_{1-x}/n-Si phototedector were prepared by chemical spray pyrolysis (CSP) technique under ambient atmosphere, when the different Mg-contents (0,30,50,70,and 90)%, temperature (450)^oC, and under pressure nitrogen (4.5)bar. X-ray diffraction (XRD) is one of the most powerful techniques for qualitative and quantitative analysis of crystalline composites. This technique has long been used to determine the general structure of solids such as thin films, including crystalline, size lattice constants, interplanar spacing, orientation of crystals (single or polycrystalline),defects, etc. The X-ray scans are performed between 2θ values of (20°-60°). The FESEM study carried out by (S-4300 of Hitachi, S-4700 FESEM in Islamic republic of Iran/ university of Tehran/ Razi foundation) scanning electron microscope equipped with energy dispersive X-ray spectroscopy (EDS). The operation principle of an AFM- type (Nanoscope III and dimension 3100) the consists of a cantilever and a sharp tip at its end. The distance between the sample surface and the tip is short enough, to allow the van der Waals forces between them to cause deflection of the cantilever. Typically, the deflection is measured using a laser spot reflected from the back surface of the cantilever into an array of photodiodes. Photocurrent is one of the most important parameter in the spectral responsivety (R_λ), quantum efficiency (Q.E), specific detectivity(D*), and noise equivalent power(NEP).Spectral resopnsivity of MgxZnO1-x /n-Si photodetector was measured using the system which is consisted of monochrometer in the range (400-1000) nm, electrometer and powermeter for measuring the radiation power for each wavelength and d.c power supply to supply bias voltage on each side of the detector this was measured in the university of Baghdad/ college of science department of physics. From the (R_λ),(Q.E),(D*),(NEP),and detectivity(D),were obtained using equations (1,3,7, and 8) respectively.

IV. STRUCTURE PROPERTIES

Structural characteristics depended on knowledge of materials and their characteristics, in order to understand how to use the different materials which include:

1. X-ray diffraction (XRD) analysis of Mg_xZnO_{1-x}/n-Si thin films

Figs.(1a,1b,1c,1d,and 1e) shows the XRD spectrum of ZnO thin films grown on silicon substrate with different Mg-contents(0,30,50,70,and 90)%,and substrate temperature (450) ^oC. There are three prominent diffraction peaks viz. (100), (002), and (101) which corresponding to different angle(31.65^o, 34,5^o, and 36.31^o), respectively belong to the hexagonal wurtzite structure of ZnO as shown in Fig.1a. It can be concluded that the thin films deposited in these experimental conditions show strong c-axis (002) orientation growth. When mixing Mg-content ratios referred to previously, and when certain conditions arise, there are three phases, the first phase remains structure of the hexagonal wurtzite, but down the intensity of the diffraction peaks as in the Fig.1b, the second phase turns into a mixture of MgO is incorporated with ZnO as in the

Fig.1c, the third phase turns into the cubic rock salt structure for the appearance of MgO diffraction peaks are clear as shown in the Figs.(1d, and 1e). In the first case,(i.e. when the Mg-content ratio (30)%) do not show any peaks additional, while in the second case, (i.e. when the Mg-content (50)% we note the appearance of two peaks two additional with directions(111), and (200) corresponding to the angles of diffraction ($36.87^o$and 42.85^o), respectively. While in the third case,(i.e. when the Mg-contents 70 and 90)% we note to increase the intensity of new peaks and the weakness of ZnO peaks and then vanish, these results are consistent with research [5]. It remains to refer to the diffraction peaks with increase ofMg-content shifted toward larger angles.

2. Field emission scanning electron microscopy (FESEM) for Mg_xZnO_{1-x}/n-Si heterojunction

The composite Mg_xZnO_{1-x}/n-Si films were measured nanostructure in the Islamic republic of Iran/ university of Tehran/ Razi foundation. Surface morphologies of (FESEM) images and their corresponding (EDS) spectra at different Mg-contents(0,30,50,70 and 90)%, and temperature of (450) °C are shown in the Figs.(2A,2B, 2C,2D, and 2E) respectively, were all fixed thickness of the films(80)nm. In addition, the measurement of concentration ratio of (30)%, at temperature (450)°C (best ratio of concentration). The morphology of the surface of pure ZnO is a nanostructure cannot determine its kind, as irregular in shape, as shown in Fig.2A. From the (FESEM) images the grain size values are found to be in the range of (30-63)nm. When you add certain compensatory ratios of Mg-content into ZnO reduced surface roughness gradually as shown in Figs.(2B, 2C,2D, and 2E). Decrease the grain size in the range of (26-54, 21-43,26- 58,15-24)nm corresponding to the concentrations of Mg-contents (30,50,70,and 90)%, respectively. These results are comparable with other results [5,6]. Grains with large sizes of (100) nm and above represent drops of material deposited in the film, which is considered as a latent defect in the film and this seems obvious when the ratio (90)% of Mg-content.

3. Elemental analysis for Mg_xZnO_{1-x}/n-Si heterojunction

The energy-dispersive X-ray analysis (EDS) spectra of the Mg_xZnO_{1-x}/n-Si thin films at (450) ^oC by (CSP) technique with different Mg-contents (x)% are given in Figs.(2a, 2b, 2c, 2d, and 2e). Among the above ratios, the ratio (30)% is the best. Which show that all the films contain the elements (Si, N, O, Zn, and Mg) as expected, indicating formation of the Mg_xZnO_{1-x} films. Fig.2a shows the (EDS) spectra of the ZnO/n-Si film and it reveals that the compound percentage for the (Si, N, O, and Zn) are (73.16, 4.64 ,12.26, and 9.94) respectively. Fig.2b depicts the (EDS) spectra of the $Mg_{0.3}ZnO_{0.7}$ film with compound percentage for the (Si, N, O, Zn, and Mg) are (72.29,6.82,10.55,6.64,and 3.70) respectively these results are comparable with other results [7,8]. The remaining percentages listed in Table1. The (EDS) spectrum for all films are clearly observable (SiKα ,ZnLα, MgKα, OKα and NKα lines). Lines did not show ZnKα, ZnKβ in the (EDS) spectra. The adhesion between the MgZnO species and the Si substrate was strong , resulting in higher growth speed in the vertical direction, was the reason why the grain size of MgZnO nanoparticles was lower than those on the Si [9]. Which led to increase the intensity of spectral lines by adding Mg-content.

Table1: Compound percentages of the Mg_xZnO_{1-x}/n-Si heterojunction.

MgO contents	Compound percentage (%)					Total
	Si	N	O	Zn	Mg	
ZnO (pure)	73.16	4.64	12.26	9.94	0	100
$Mg_{0.3}ZnO_{0.7}$	72.29	6.82	10.55	6.64	3.70	100
$Mg_{0.5}ZnO_{0.5}$	74.09	3.92	11.60	3.55	6.84	100
$Mg_{0.7}ZnO_{0.3}$	73.67	4.57	11.66	1.40	8.70	100
$Mg_{0.9}ZnO_{0.1}$	73.18	4.69	12.16	0.52	9.45	100

4. AFM for Mg_xZnO_{1-x}/n-Si heterojunction

Fig.3 shows the surface topography of the thin films. It shows 3-D and granularity accumulation distribution of AFM images for the Mg_xZnO_{1-x}/n-Si thin films at different Mg-content (x), at substrate temperature $(450)^oC$, and nitrogen pressure (4.5) bar, with scanning area (2000×2000) nm^2. From figures shown can that describe the general appearance of the Mg_xZnO_{1-x} films prepared, as are deposited vertical to the surface of the substrate silicon is made up of nanorods (NRs), and when increasing the Mg-content in the lattice ZnO line up the rails and turns into the nanowalls (NWs) as shown in the pictures. It can identify the parameters that can be found through AFM technique are the average diameter, the total number of granules, surface thickness, roughness average, the root mean square (RMS) of the average of roughness, and the average of height. We note average increase diameter with increasing Mg-content, which leads to a decrease grain size, and this is due to the Mg ion radius smaller than the radius of the Zn ion, these results are listed in Table2. These results are comparable with other results [10] . The roughness average decreases randomly when the Mg-content ratio (90)% to increase substantially, and is attributed to the dominance of the Mg-content in the lattice of Zn and a phase transition to the cube structure and this is reflected on the (RMS), where it depends on the roughness average and to behaves the same behavior. While the height average is the other exhibits the same behavior (RMS). The best Mg-content ratio is (30)%.

Table2:The average diameter, total grain No., surface thickness, roughness average, root mean square, and average height for Mg_xZnO_{1-x}/n-Si thin films at different Mg-content (0,30,50,70, and 90)%, and at temperature (450) °C.

Silicon substrate	Substrate temperature (450) °C, thickness =(80) nm					
Sample	Average diameter (nm)	Total grain No.	Surface Thickness (nm)	Roughness (nm)	RMS (nm)	Average height (nm)
ZnO (pure)	69.57	287	3.87	0.742	0.850	0.679
$Mg_{0.3}ZnO_{0.7}$	98.31	175	1.41	0.228	0.264	0.220
$Mg_{0.5}ZnO_{0.5}$	93.99	122	3.83	0.617	0.719	0.617
$Mg_{0.7}ZnO_{0.3}$	100.83	119	1.60	0.319	0.367	0.299
$Mg_{0.9}ZnO_{0.1}$	101.10	114	6.00	1.150	1.320	1.088

V. FIGURES OF MERIT FOR Mg_xZnO_{1-x} /n-Si PHOTOCONDUCTIVE DETECTORS

The responsivity (R_λ) of Al/Mg_xZnO_{1-x}/n-Si/Al heterojunction detectors with different Mg-contents (x)%, and at the temperature (450)°C to the proportion for Mg-content (30)% calculated by using equation(1). The (R_λ) of Al/Mg_xZnO_{1-x}/n-Si/Al photodetectors increases with increasing Mg-content measured for white light and bias voltage equal to (3Volt) for ratio (30)% of Mg-content only. Fig.4a shows (R_λ) change as a function of wavelength for Al/Mg_xZnO_{1-x}/n-Si/Al films. It is clear from figure that there are two regions of the peaks response, the first region is located at visible spectrum (450)nm, and the second located at near infrared spectrum (NIR)(900) nm. The result of (R_λ) means that the portion of light with higher energy, such as (450) nm, is absorbed by MgZnO layer (region one) and the portion of light with lower energy, such as (900) nm (region two), can completely incident into n-Si substrate and is absorbed. These results are due to the absorption edges MgZnO and n-Si. At short wavelength incident photon energy which is larger than the energy gap indicates a large increase in the (R_λ) and this increase relates to the high absorption coefficient. The (R_λ) of the ratio of Mg-contents (50,70, and 90)% are more decrease, is due to increment of the barrier height and decrement of the absorption coefficient. Quantum efficiency(QE) is a very important criterion in the photovoltaic devices which is known as optoelectronic effect, it represents the ratio between the numbers of generating electrons in the hetrojunction to the number of incident photons on the effective area of the hetrojunction.(QE) is related to the change of the spectral responsivity were calculated using equation(3). (QE) was determined as a function of wavelength for Mg_xZnO_{1-x}/n-Si photoconductive detectors, as shown in Fig.4b for different Mg-content. It is observed that $Mg_{0.3}ZnO_{0.7}$/n-Si photodetector with(30)% from Mg-content has higher quantum efficiency comparing to the photodetectors for the remaining percentages of the Mg-content due to the lowest barrier height and highest photocurrent. Fig.4c show the variation of specific detectivity (D*) as a function of wavelength for Mg_xZnO_{1-x}/n-Si hetrojunction at different Mg-content of (x)% ,and temperature (450)°C were calculated using equation (7). We can notice that the (D*) value increases with increasing Mg-content, due to the improvement in the structural and electrical properties of this hetrojunction. Increasing Mg-content to reduce structural defects and thus reducing the recombination and reduce the noise generated in the current detector center and as a result increase significantly the (D*).The noise equivalent power (NEP) values were calculated using equation (8) as shown in Fig.4d for Mg_xZnO_{1-x}/n-Si heterojunction at different Mg-content of (x)%. We can observe that the minimum (NEP) occurs when (R_λ) has the maximum value as shown in Fig.4a. From this figure we can notice that (NEP) decreases with increasing of Mg-content.

VI. CONCLUSIONS

Briefly,Mg_xZnO_{1-x} heterojunction have been prepared on n-Si substrate by chemical spraying pyrolysis (CSP) technique, and an metal semiconductor metal (MSM) structured photodetector was fabricated based on the film. There are two regions of the peaks response, the first region is located at visible spectrum, and the second located at near infrared spectrum (NIR).The responsivity, quantum efficiency and specific detectivity decreases in visible region and increase in (NIR)with increasing of Mg-content.(NIR) of the increase in high concentrations of Mg-content. We believe that much improvement in the performance of the photodetector can be attained by suppressing the phase separation of Mg_xZnO_{1-x}. The results obtained in this paper confirm that Mg_xZnO_{1-x} can be a strong candidate for photodetector applications.

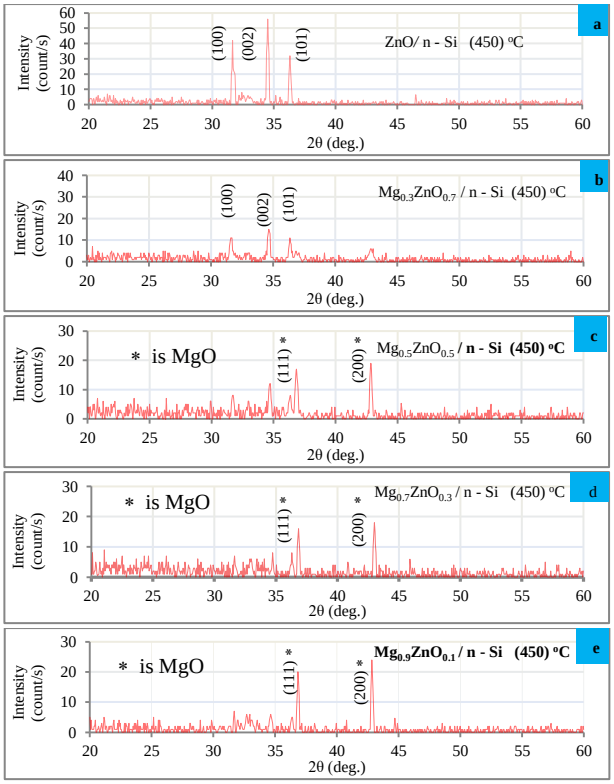

Fig.1: XRD patterns for Mg_xZnO_{1-x}/n -Si heterojunction with different Mg-content (0,30,50,70,and 90)% and at (450) °C.

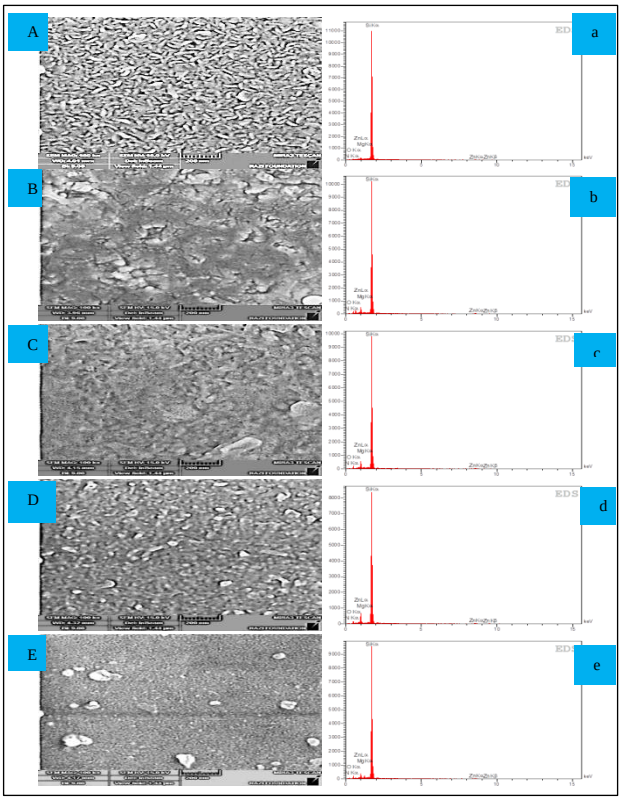

Fig.2:FESEM and EDS for Mg_xZnO_{1-x} /n-Si heterojunction for Mg-content (x)% prepared at substrate temperature(450) ^oC.

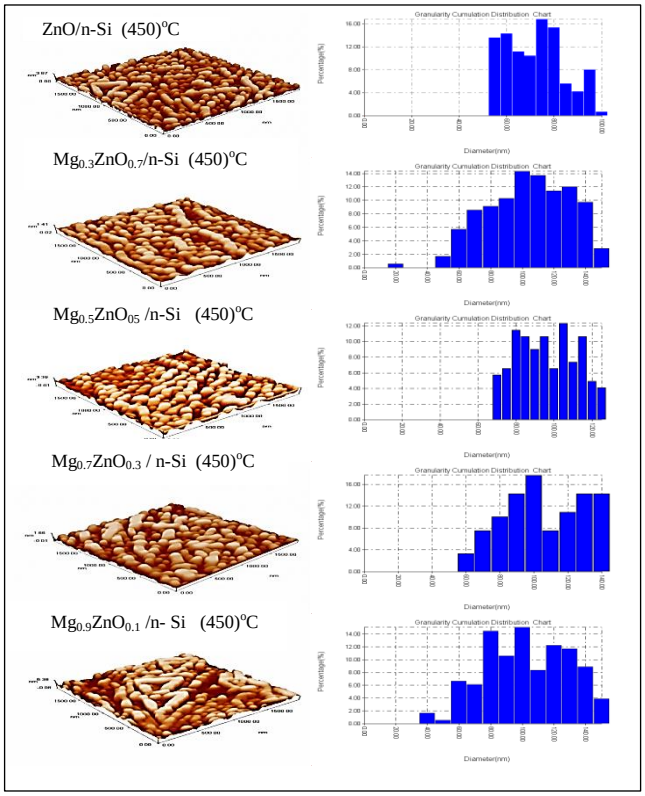

Fig.3: 3-D AFM image and granularity accumulation for Mg_xZnO_{1-x} /n-Si heterojunction with different Mg-content (0, 30, 50, 70, and 90)% and at temperature (450) ^oC.

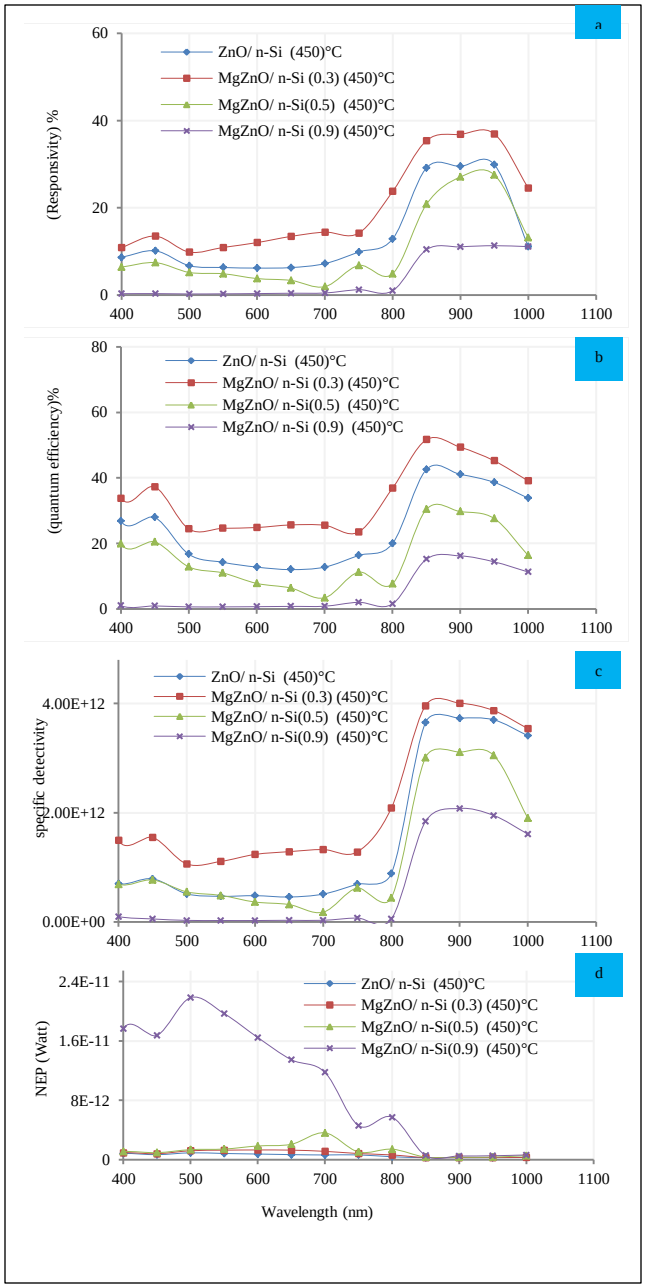

Fig. 4: The variation of responsivity, quantum efficiency, specific detectivity, and noise equivalent power as a function of wavelength for Mg_xZnO_{1-x}/n-Si heterojunction at different Mg-content.

First Author: Abdulazeez O. Mousa

Department of Physics, College of Science, University of Babylon, P.O. Box 4, Babylon, Iraq
E-mail address: *Azizliquid_2005@yahoo.com

Second Author: Saleem H. Trier

Department of Environment, College of Science, University of Al- Qadisiyah, Diwaniya, Iraq
E-mail address: * Salemhamza79@yahoo.com

REFERENCES

[1] E. M. Nasir,"Fabrication ofCdSe: Cu photoconductive detector by using vacuum evaporation technique and studying its electro-optical properties",M.Sc. thesis, University of Baghdad, dep. of physics, (1999).

[2] M. Caria, L. Barberini, S. Cadeddu, A. Giannattasio, A. lia, A. Rusani, and A. Sesselego, "Far UV responsivity of commercial silicon photodetectors", J. of nuclear instruments and methods in physics research A, Vol. 466, pp.(115-116), (2001).

[3] R. Ionenescu, A. Vancu," Time-dependence of the conductance of SnO_2:Pt:Sb in atmospheres containing oxygen, carbon monoxide and water vapour I. Non-oscillatory behavior", Applied Surface Science, Vol.74, pp.(207-212), (1994).

[4] D. Song, "Effect of RF power on surface- morphological, structural and electrical properties of aluminum-doped ZnO films by magnetron sputtering", Applied surface science, Vol. 254, pp.(4171-4178) , (2008).

[5] M. Su Kim, K. Tae Noh, K. Gug Yim, S. Kim, G. Nam, D.-Yul Lee, J. Soo Kim, J. Su Kim, and J.-Young Leem, "Composition dependence on structural and optical properties of $Mg_xZn_{1-x}O$ thin films prepared by Sol-Gel method", Bull. Korean Chem. Soc.,Vol.32, p.3458, (2011).

[6] D. Raoufi, and T. Raoufi, "The effect of heat treatment on the physical properties of sol-gel derived ZnO thin films",Appl. Surf. Sci. Vol.255, pp.(5812-5818), (2009).

[7] P.S. Shewale, and Y.S. Yu, "Structural surface morphological and UV photodetection properties of pulsed laser deposited Mg-doped ZnO nanorods effect of growth time", Journal of Alloys and Compounds,Vol.654, pp.(79-86), (2016).

[8] H. Seung Kim, C. H. Kim, and L. Yue , "A study of the growth of single-phase $Mg_{0.5}Zn_{0.5}O$ films for UV LED", International Journal of Chemical, Nuclear, Materials and Metallurgical Engineering Vol.8, (2014).

[9] R. Cusco, E. Alarcón Lladó, J. Ibáñez, and L. Artús, "Temperature dependence of Raman scattering in ZnO", Physical Review B75, p.165202 ,(2007).

[10] S. Shanmugan, D. Mutharasu, I. Abdul Razak,"Sol-Gel derived Mg and Ag doped ZnO thin film on glass substrate", Structural and Surface Analysis, Journal of Optoelectronics and Biomedical Materials Vol.6, pp.(119-129) , (2014).